# PROJETO DE TRANSDUTOR DE PRESSÃO DE SEMICONDUTOR DE DIAMANTE

# DESIGN DIAMOND SEMICONDUCTOR PRESSURE TRANSDUCER

# КОНСТРУКЦИЯ АЛМАЗНОГО ПОЛУПРОВОДНИКОВОГО ДАТЧИКА ДАВЛЕНИЯ

AFANASYEV, Sergey A.[1*]; AFANASYEV, Mikhail S.[2]; FESHCHENKO, Valery S.[3]; LVOV, Sergey A.[4]; ZHUKOV, Alexander O.[5]

[1, 2] Moscow Technological University (MIREA), Department of Metrology and Standardization
78 Vernadsky Ave., Zip code 119454, Moscow – Russian Federation
(phone: +89067987572)

[3,4] LLC PTC "Ural AlmazInvest"
4 Ivan Franko Str., Zip code 121108, Moscow – Russian Federation
(phone: +89031467246)

[5] State Astronomical Institute named after P.K. Shternberg Moscow State University, Institute of Astronomy of the Russian Academy of Sciences
13 Universitetskiy Ave., Zip code 119234, Moscow – Russian Federation

** Corresponding author*
*e-mail: michaela2005@yandex.ru*

Received 01 December 2017; received in revised form 08 June 2018; accepted 09 July 2018

## RESUMO

Os sensores de pressão desempenham um papel importante na medição de variáveis nos sistemas de controle e automação de vários processos. O objetivo deste artigo é estudar o projeto de um sensor de pressão de semicondutor de diamante. Para atingir esse objetivo, a análise foi baseada na Lei de Fourier, mas os autores fizeram mudanças no modelo de equações. O estudo foi realizado utilizando diamantes, pois são dos materiais promissores para a fabricação de sensores e possuem grande robustez, resistência térmica e a radiação. Foi estabelecido que a corrente de saída em um semicondutor não depende da tensão de alimentação. Ao determinar a resistência de isolamento entre as placas do sensor, determinou-se que a resistência é menor que 200 MW e que atende aos requisitos técnicos.

**Palavras-chave**: *pressão de materiais, materiais de diamante, modelo matemático, tecnologia de semicondutores*

## ABSTRACT

Pressure sensors play an important role in measuring variables in the control and automation systems of various processes. The purpose of this article is to study the design of a diamond semiconductor pressure sensor. In order to achieve this goal, the analysis was based on the Fourier law, but the authors made changes in the model of equations. The study was carried out using diamonds, as they are one of the promising materials for the manufacture of sensors and have high strength, thermal and radiation resistance. It was established that the output current in a semiconductor converter of the same load on the membrane does not depend on the supply voltage, which corresponds to the technical requirements developed in the converter. When determining the insulation resistance between the sensor plates, it was determined that the insulation resistance is less than 200 MW that meets the technical requirements.

**Keywords:** *pressure of materials, diamond materials, mathematical model, semiconductor technology.*





DOI: 10.52571/PTQ.v15.n30.2018.691_Periodico30_pgs_687_695.pdf

## АННОТАЦИЯ

Для измерения переменных в системах управления и автоматизации различных процессов важную роль играют датчики давления. Целью данной статьи является изучение конструкции алмазного полупроводникового датчика давления. Для достижения поставленной цели проводился анализ на основе закона Фурье, но авторами были внесены изменения в модели уравнений. Исследование проводилось с использованием алмазов, поскольку они являются одним из перспективных материалов для изготовления датчиков и имеют высокую прочность, термическую и радиационную стойкость. Установлено, что выходной ток в полупроводниковом преобразователе той же нагрузки на мембране не зависит от напряжения питания, которое соответствует техническим требованиям, разработанным в преобразователе. При определении сопротивления изоляций между пластинами датчика было установлено, что сопротивление изоляций составляет менее 200 МВт, что соответствует техническим требованиям.

**Ключевые слова:***давление материалов, алмазные материалы, математическая модель, полупроводниковая технология.*

## INTRODUCTION

In modern technology, widespread of the semiconductor capacitive and inductive pressure sensors. The need to preserve high metrological and operational characteristics of the sensors t in the conditions of toughening of the requirements of the external influencing factors requires the application of new materials for the manufacture of sensitive elements (SE), so pressing is the task of finding a material superior silicon on mechanical and electrophysical parameters (Mikhailenko *et al.*, 2017; Khazan and Gorodetskii, 1967). First, such materials include diamond, which is a wide-gap semiconductor with a band gap of 5.4 eV.

The diamond PP is developed based on microelectromechanical systems based on diamond and integrated circuits CAV444 and AM402 production of Analog Microelectronics (Germany), using a minimum number of external discrete components.

A functional diagram of the capacitive PP is presented in figure 1.

Part PP includes capacitive microelectromechanical system (MEMS) capacitance change which depending on the external pressure is converted into an electric voltage with a voltage Converter the capacitance-to-voltage. Design, manufacturing technology and theoretical bases of its functioning are described in (Altukhov *et al.*, 2017a; Altukhov et al., 2017b).

The output voltage is fed to the input node of the Converter voltage – current, which provides an output current capacitive PP 4..20 mA.

On the basis of the functional diagram of PP developed a schematic diagram of the capacitive PP, which is presented in figure 2.

Schematic diagram complies with the manufacturer's recommended. MEMS is connected to terminals 1 and 2 of the Board and is connected to the input 12 of the chip CAV444 (Agrawal, 2017; Prelas *et al.*, 2016; Ask and Öberg, 1979; Igamberdiev *et al.*, 2002). The differential output signal from its outputs 5 and 6 arrives at the inputs 8 and 9 of IC AM402. Resistors R4 – R11 is intended to adjust the gain and offset voltage of the output signal. The transistor VT1 in conjunction with resistor R12 provide the desired output current PP. The diode VD1 is designed to protect the circuit from reverse polarity voltage.

CAV444 chip is a chip of the transducer capacitance-to-voltage. The voltage at the IC output proportional to input capacitance. CAV444 can be used as a capacitance-to-voltage with a differential output or as a pre-cascade device with high functionality such as converters capacitance-current and capacitance code (Katkov *et al.*, 2011; Pavese and Molinar, 1992; Kedrinskii *et al.*, 1969). A wide range of capacitance and high sensitivity allows the chip to use it in various fields of technology and electronics.

The output voltage at pin 5 relative to the earth is a linear function of the capacitance CM. To convert the output voltage CAV444 to the desired output current PP is a chip AM402. IC AM402 represents an integrated circuit of the Converter current, which is specifically designed

for processing differential signals.

AM402 is designed for two - and three-wire inclusions and includes the following functional blocks:

– the input stage, which is used as a measuring amplifier of high accuracy (IA);

– voltage reference, the adjustable output voltage from 4.5 V to 10V, designed to power internal circuits and external components;

– voltage-controlled current amplifier that can generate output currents which correspond to industrial standards (0 / 4-20 mA, 12 ± 8 mA).

For the chip as a Converter of current output requires an external transistor, which reduces the power dissipation of the chip, and the diode that protects the transistor from reverse polarity of the supply voltage and external resistors (Egorov *et al.*, 2016; Mourzina *et al.*, 2004; Handa *et al.*, 1975). Changing a few external components, the output current can be changed in a wide range. IC AM402 has surge protection at the input, this disables the output current. Another safety feature included in AM402 is a function of power off in high temperature. In this case the output current off if the temperature of the chip exceeds 150 °C.

Diamond is a semiconductor pressure transducer, the design allows you to measure pressure with high accuracy and stability (Milnes, 1980).

To clarify the parameters and verify characteristics of diamond PP was produced according to the procedures developed following studies:

1. Verification of pressure measuring range.
2. Check the range of the output current.
3. Check supply voltage range.
4. Measurement of output capacity of PP.
5. Check variation and repeatability of the output signal.
6. Check the stability of the output signal during the year.
7. Check the insulation resistance between the plates of the sensor.
8. Check the insulation resistance between the sensor plates and the housing.
9. Test electric strength between the plates of the sensor and the housing.
10. Check the operating temperature range of the MEMS.

## MODELING FRAMEWORK TO PREVENT DEFORMATION:

If we talk about basic equations, they are as follows (Equation 1 – Equation 5). When the processes that occur at high temperatures and are of the nature of anomalous warmth has spread with finite speed (Equation 6). Substituting the value of heat flux density (Equation 7) in the balance equation of heat for a one-dimensional problem (Equation 8) get the hyperbolic equation of heat transfer. If the power density of heat sources W = 0, equation (2) can be written as Equation 9.

Comparing with the classical law of heat conduction Fourier transform, we see that when the finite speed of propagation of heat in the heat conduction equation should be replaced $\frac{\delta T}{\delta t}$ in the amount of $\frac{\delta T}{\delta t} + \tau_0$.

As a result, the system of equations (Equation 1) linking $\sigma_x T, B,$ takes the form Equation 10 – Equation 13. Here Equation 14. To simplify the system of related Equation 3 – Equation 5 omit the nonlinear member in Maxwell's equation for magnetic induction Equation 15. This simplification applies if B does not depend on deformation and temperature. Thus, the magnetic flux density satisfies the diffusion Equation 15.

The solution of equation Equation 6 is known and for the case of the stepping task on the border x = 0 (Equation 16) magnetic induction in the half-space x ≥ 0 is given by Equation 17, where Equation 18. Using well-known equations for the error functions (Equation 19). Thus, the magnetic induction in this model becomes a source of disturbances in the associated equations of thermoelasticity.

Inserting in equation Equation 3, Equation 4 the dimensionless quantities (Equation 20 – Equation 22) obtained for the considered problem the following system of Equation 23, Equation 24 with the initial conditions (Equation 25) and boundary conditions (Equation 26). In the General case, the temperature field must satisfy the conditions of convection. However, in this work, the convection on the surface ξ = 0 is taken equal to zero. Magnetic induction, which enters into the Equation 8, Equation 9 is determined using the expression (Equation 27).

Unknowns and the parameters that

correspond to mechanical properties of the particular layer 1 or 2 in the future, if necessary, will be marked by a subscript i (i=1,2).

If the layer is not conductive, the system Equation 8 and Equation 9 suppose β = 0 and consider the termoparnaya problem with the initial conditions (10), boundary mechanical (Equation 28) and boundary thermal conditions (Equation 29). Here $q = -\bar{q}$ , $\bar{q}$ – the heat flux density in the direction of the external normal to the surface $\xi = 0$ ; $f(\tau)$ and $\varphi(\tau)$ – specified laws change loads.

Also, take into account the matching conditions at the interface of layers which are equal in stresses and displacements, temperatures and heat fluxes.

## METHODS AND RESULTS OF THE EXPERIMENT:

Research trials of experimental samples of diamond PP were conducted according to the following techniques:

*1. Verification of pressure measuring range.* Experimental study of characteristics of PP was carried out on a special stand, which includes: the device is calibrated vertical force (CEF); power supply with adjustable output voltage; multimeter Agilent U-1241B.

A special device calibrated vertical force (CEF) is used to create discrete concentrated forces. KVU is the bowl (platform), on which is placed the load is known in advance of the mass, simulating a concentrated force P (Guha *et al*., 1979; Or and Chan, 2008). In the Central part of the lower side of the dispenser is connected to the rod. The device is placed on the precision of probe movement. A cross-sectional view of the device of IEDs is presented in figure 3.

In a stationary glass 1 device is movable needle 3 placed on one end of the needle of the court 2 for the calibrated load. The weight of the needle without load is 0,9332 grams. The site can accommodate a weight of 200.0 grams. Upon contact of the needle device, where membrane of PP, the weight is completely transferred to the membrane, causing its deflection proportionally to the weight of the cargo. PP was included in the measuring circuit shown in figure 4.

The measurement of PP was performed using a device calibrated vertical force by the following procedure: a multimeter was included in the position measuring DC current with a range to 20 mA; set output voltage of power supply 24 V; measured output current of the PP in the original unloaded state.

Further, the measured output current of the PP under the influence of external pressure for which the device KVU was raised on a platform device, where the goods were placed with a fixed mass.

Membrane loaded needle with a load of 200.0 g and a measured output current PP. Output current PP in the initial state was equal to 4 mA, and the load is 20 mA, which fully complies with the requirements of the investigated diamond PP.

*2. Check the range of change of the output current.* Before testing the PP was installed and mechanically fixed on the stand so that the PP membrane was positioned horizontally and its center was opposite the needle, where. PP was included in the measuring circuit shown in figure 4 (Kenigsberg *et al*., 1978; Hierlemann and Baltes, 2006).

The measurements of the output current PP: with the load increasing from 1.0 gram to 200.0 grams; with the load decreasing from 200,0 gram to 1.0 gram. Output current PP changed from 4 mA to 20 mA, fully complies with the requirements.

*3. Check supply voltage range*. The PP test was conducted at voltages of a power source 7.5 V, 12 V, 18 V, 24 V, 30 V, 36 V, with load values on the membrane equal to 20 g and 200 g. Output current PP of the same load on the membrane is not dependent on the supply voltage that meets the technical requirements developed by PP.

*4. Measurement of output capacity of PP.* Measurement of output capacity of PP was carried out using the RLC meter E7-8, a measuring probe which is connected to the output terminals of the MEMS PP. The capacitance between the output terminals of the MEMS of PP did not exceed 17 pF.

*5. Check variation and repeatability of the output signal.*PP was included in the measuring circuit shown in figure 4. Conducted five series of experiments measuring the output current PP: with the load increasing from 1.0 gram to 200.0

grams; with the load decreasing from 200,0 gram to 1.0 gram. The difference between the output currents of PP under the same loads in all five series of experiments does not exceed 1.2 %.

*6. Check the stability of the output signal during the year.* Output stability during the year was tested as follows. PP was tested according to the test procedure of pressure measuring range. The test was repeated once a week throughout the year. The difference between the output currents of PP under the same loads in all experiments did not exceed 0.7 %, which fully complies with the requirements of the investigated diamond PP.

*7. Check the insulation resistance between the plates of the sensor.* Check the insulation resistance between the plates of the sensor was carried out using a multimeter Agilent U-1241B.

The results of the experiment showed that the insulation resistance between the electrodes of the sensor is not less than 200 MW, which corresponds to the technical requirements developed by PP.

*8. Check the insulation resistance between the sensor plates and the housing.* Check the insulation resistance between the sensor plates and the shell was carried out using the Agilent multimeter U-1241B.

The results of the experiment showed that the insulation resistance between each of the electrodes of the sensor and sensor housing of at least 20 MW, which corresponds to the technical requirements developed by PP.

*9. Test electric strength between the plates of the sensor and the housing.* Test electric strength between the plates of the sensor and housing were carried out using a megger M4100/3 at the test voltage of 500 V.

The results of the experiment showed that the insulation resistance between each of the electrodes of the sensor and sensor housing of at least 20 MW, which corresponds to the technical requirements developed by PP.

*10. Check temperature range MEMS.* Testing of a MEMS diamond PP on the impact of high and low temperature was carried out by GOST 20.57.406–81 at ambient temperatures - 40° C and + 125° C.

The results of the experiment showed that under the given ambient temperature MEMS diamond PP is fully functional and retains its specifications.

## CONCLUSION

Developed and studied in this work, diamond is a semiconductor Converter (PP) pressure is of undoubted scientific and practical interest. Diamond is one of the most promising materials for the fabrication of sensors. It is associated with such properties as high strength, large band gap, high electrical strength, high thermal and radiation resistance of the diamond crystals.

The obtained results allow to conclude about the viability and reliability of the original development of MEMS technologies based on diamond materials to create transducers the new type, and further applied in future types of spacecraft, information and automated control systems for transport and space systems.


## ACKNOWLEDGEMENTS:

The work is executed at financial support of the Ministry of education and science of the Russian Federation (agreement No. 14.577.21.0177, a unique identifier of applied research RFMEFI57715X0177).


## REFERENCES:


1. Agrawal, D.P. *Different Types of Transducers Embedded Sensor Systems*, Singapore: Springer Singapore, 2017.
2. Altukhov, A.A., Gladchenko, E.V., Feshchenko, V.S. *STIN*, **2017a**, 1, 25 – 28.
3. Altukhov, A.A., Gladchenko, E.V., Feshchenko, V.S. *STIN*, **2017b**, 2, 32 – 36.
4. Ask, P., Öberg, P.Â. *Medical and Biological Engineering and Computing*, **1979**, 17(3), 360-364. doi:10.1007/bf02443823
5. Egorov, F.A., Potapov, V.T., Melkumov, M.A., Amelichev, V.V., Generalov, S.S., Shamanaev, S.V. *Technical Physics Letters*, **2016**, 42 (5), 501-504. doi:10.1134/s1063785016050242
6. Guha, S.K., Anand, S., Tandon, P.N. *Medical and Biological Engineering and Computing*, **1979**, 17 (6), 757-762. doi:10.1007/bf02441558

7. Handa, H., Yoneda, S., Matsuda, M., Handa, J. A *Miniature SFT Transducer for Continuous Monitoring of Intracranial Pressure. Intracranial Pressure II,* Berlin. Heidelberg: Springer Berlin Heidelberg, 1975.
8. Hierlemann, A., Baltes, H., *Semiconductor-Based Chemical Microsensors, MEMS: A Practical Guide to Design, Analysis, and Applications.* Berlin, Heidelberg: Springer Berlin, 2006.
9. Igamberdiev, K.T., Onarkulov, K.É., Rasulov, R.T., Yusupova, D.A. *Journal of Engineering Physics and Thermophysics*, **2002**, 75(6), 1329-1331. doi:10.1023/a:1022158724974
10. Katkov, A.N., Novikov, V.N., Chuvykin, B.V.*Measurement Techniques*, **2011**, 54(54), 428. doi:10.1007/s11018-011-9743-7
11. Kedrinskii, V.K., Soloukhin, R.I., Stebnovskii, S.V. *Journal of Applied Mechanics and Technical Physics*, **1969**, 10(4), 607-610. doi:10.1007/bf00916219
12. Kenigsberg, V.L., Stuchebnikov, V.M., Serdyukov, V.I., Evdokimov, V.I., Sukhodolets, V.K., Mil'man, S.I. *Measurement Techniques*, **1978**, 21(10), 1457-1460. doi:10.1007/bf00823096
13. Khazan, A.D., Gorodetskii, A.F. *Biomedical Engineering*, **1967**, 1(2), 99-102. doi:10.1007/bf00557545
14. Mikhailenko, I.V., Orlov, A.T., Serdega, B.K. *Semiconductors*, **2017**, 51(4), 498-502. doi:10.1134/s1063782617040145
15. Milnes, A.G. *Semiconductor Sensors and Transducers Semiconductor Devices and Integrated Electronics*, Dordrecht: Springer Netherlands, 1980.
16. Mourzina, I.G., Yoshinobu, T., Ermolenko, Y.E., Vlasov, Y.G., Schöning, M.J., Iwasaki, H. *Microchimica Acta*, **2004**, 144(1), 41-50. doi:10.1007/s00604-003-0091-4
17. Or, S.W., Chan, H.L.W. *Piezocomposite Ultrasonic Transducers for High-Frequency Wire Bonding of Semiconductor Packages, Piezoelectric and Acoustic Materials for Transducer Applications*, Boston: Springer US, MA, 2008.
18. Pavese, F., Molinar G. *Pressure Transducers for Gaseous Media Modern Gas-Based Temperature and Pressure Measurements*, Boston: Springer US, 1992.
19. Prelas, M., Boraas, M., De La Torre, A.F., Seelig, J.-D., Tchouaso, M.T., Wisniewski, D. *Power Density Dilution Due to the Interface of the Isotope with the Transducer Nuclear Batteries and Radioisotopes*, Cham: Springer International Publishing, 2016.


***Figure 1.*** *Functional diagram of the capacitive PP: 1 micro electro – mechanical system based on diamond; 2 – the transducer capacitance – voltage, 3 – voltage – to-current*

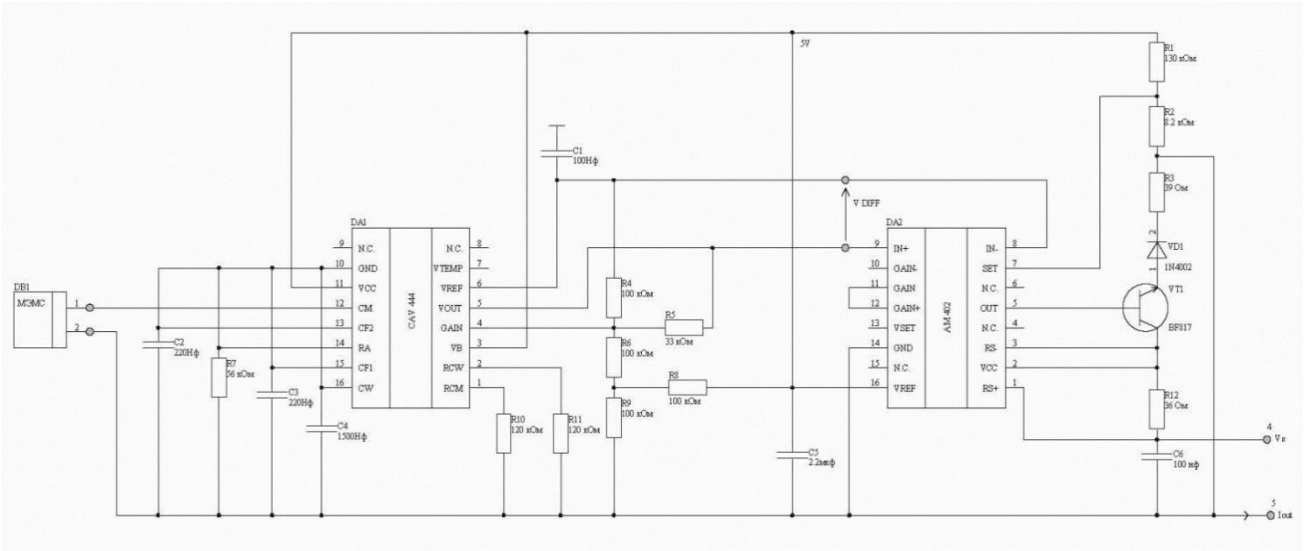

***Figure 2.*** *Schematic diagram of the capacitive PP*

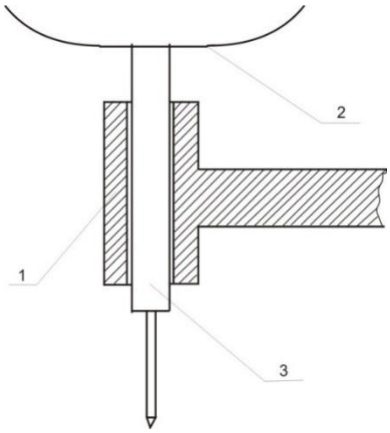


***Figure 3.*** *Cross-sectional view of the device calibrated vertical efforts*

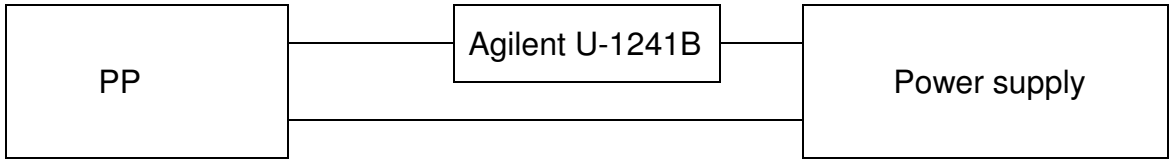


***Figure 4.*** *Scheme of the Measuring stand*

$$\rho \frac{\delta^2 u}{\delta t^2} - \frac{\delta \sigma_x}{\delta x} = f. \quad (1)$$

$$\rho \frac{\sigma T}{\sigma t} + \alpha T_0 (3\lambda + 2\mu) \frac{\delta^2 u}{\delta x \delta t} - k \frac{\delta^2 T}{\delta x^2} = g. \quad (2)$$

$$\sigma_x = (\lambda + 2\mu) \frac{\delta u}{\delta x} - \alpha (3\lambda + 2\mu) T. \quad (3)$$

$$\frac{\delta E}{\delta x} + \frac{\delta B}{\delta t} = 0, -\frac{\delta B}{\delta x} = \mu_0 J. \quad (4)$$

$$J = \sigma_0 (E - B \frac{\delta u}{\delta t}). \quad (5)$$

$$V = (\frac{k}{c_0 \rho \tau_0})^{1/2}. \quad (6)$$

$$q_x = -k \frac{\delta T}{\delta x} - \tau_0 \frac{\delta q_x}{\delta x}. \quad (7)$$

$$c_v \rho \frac{\delta T}{\delta t} = -\frac{\delta q_x}{\delta t} + W. \quad (8)$$

$$c_v \rho \left( \frac{\delta T}{\delta t} + \tau_0 \frac{\delta^2 T}{\delta t^2} \right) = k \frac{\delta^2 T}{\delta x^2}. \quad (9)$$

$$\frac{\partial^2 \sigma_x}{\partial x^2} - \frac{1}{c^2} \cdot \frac{\partial^2 \sigma_x}{\partial t^2} = \alpha \rho \frac{1+\nu}{1-\nu} \cdot \frac{\partial^2 T}{\partial t^2} + \frac{1}{2\mu_0} \cdot \frac{\partial^2 B^2}{\partial x^2} \quad (10)$$

$$\frac{\partial^2 T}{\partial x^2} - \frac{1}{V^2} \cdot \frac{\partial^2 T}{\partial t^2} = \frac{1}{a}(1+\varepsilon) \cdot \frac{\partial T}{\partial t} + \frac{\alpha T_0}{\kappa} \cdot \frac{1+\nu}{1-\nu} \cdot \frac{\partial \sigma_x}{\partial t} + \frac{1}{\kappa \mu_0 \sigma_0} \left( \frac{\partial B}{\partial x} \right)^2 \quad (11)$$

$$\frac{\partial^2 B}{\partial x^2} - \mu_0 \sigma_0 \frac{\partial}{\partial x} \left( B \frac{\partial u}{\partial x} \right) = \mu_0 \sigma_0 \frac{\partial B}{\partial t} \quad (12)$$

$$c^2 = (\lambda + 2\mu)/\rho; \qquad a = \kappa / c_\nu; \qquad V^2 = a/(\rho \tau_0); \quad (13)$$

$$\varepsilon = \frac{\alpha^2 T_0 (3\lambda + 2\mu)^2}{c_\nu (\lambda + 2\mu)} = \frac{(1+\nu)\alpha^2 E T_0}{(1-\nu)(1-2\nu) c_\nu}. \quad (14)$$

$$\frac{\partial^2 B}{\partial x^2} = \sigma_0 \mu_0 \frac{\partial B}{\partial t} \quad (15)$$

$$B(0,t) = \begin{cases} B_0, t \geq 0, \\ 0, \ t < 0, \end{cases} \quad (16)$$

$$B(x,t) = B_0 \operatorname{erfc}(mx) \tag{17}$$

$$m = \frac{1}{2}\left(\mu_0 \sigma_0 / t\right)^{1/2} \tag{18}$$

$$\frac{\partial B}{\partial x} = -\frac{2B_0 m}{\sqrt{\pi}} \cdot e^{-m^2 x^2} \tag{19}$$

$$\xi = \frac{cx}{a}; \quad \tau = \frac{c^2 t}{a}; \quad \Theta = \alpha T; \quad \sigma = \frac{(1-2\nu)\sigma_x}{E} = \frac{\sigma_x}{3\lambda + 2\mu}; \tag{20}$$

$$\beta = \frac{B}{B_0}; \ \gamma = \frac{B_0^2}{2\mu_0} \cdot \frac{1-2\nu}{E}; \ \varphi = \frac{\alpha B_0^2}{k c_\nu}, \ k = a\mu_0\sigma_0; \ c_1^2 = 1; \tag{21}$$

$$c_2^2 = \frac{V^2}{c^2} \tag{22}$$

$$\frac{\partial^2 \sigma}{\partial \xi^2} - \frac{1}{c_1^2} \cdot \frac{\partial^2 \sigma}{\partial \tau^2} = \frac{\partial^2 \Theta}{\partial \tau^2} + \gamma \frac{\partial^2 \beta^2}{\partial \xi^2} \tag{23}$$

$$\frac{\partial^2 \Theta}{\partial \xi^2} - \frac{1}{c_2^2} \cdot \frac{\partial^2 \Theta}{\partial \tau^2} = (1+\varepsilon)\frac{\partial \Theta}{\partial \tau} + \varepsilon \frac{\partial \sigma}{\partial \tau} + \varphi\left(\frac{\partial \beta}{\partial \xi}\right)^2 \tag{24}$$

$$\sigma = \frac{\partial \sigma}{\partial \tau} = \Theta = \frac{\partial \Theta}{\partial \tau} = 0 \ \tau = 0, \ \xi > 0 \tag{25}$$

$$\frac{\partial \Theta}{\partial \xi} = 0, \ \beta = \begin{cases} 1, \tau \geq 0, \\ 0, \tau < 0 \end{cases} \quad \text{at} \quad \xi = 0; \ \sigma = 0 \quad \text{at} \quad \xi = 1 \tag{26}$$

$$\beta = \operatorname{erfc}\left(\frac{\xi}{2} \cdot \sqrt{\frac{k}{\tau}}\right), \ \frac{\partial \beta}{\partial x} = -\sqrt{\frac{k}{\pi\tau}} \exp\left(-\frac{k}{4} \cdot \frac{\xi}{\tau}\right) \tag{27}$$

$$\sigma = -p_0 f(\tau) \text{ when } \xi = 0; \ \sigma = 0 \text{ when } \xi = 1 \tag{28}$$

$$\frac{\partial \theta}{\partial \xi} = q\varphi(\tau) \ \xi = 0; \ \frac{\partial \theta}{\partial \xi} = 0 \ \xi = 1 \tag{29}$$